NANO LETTERS

Letter

pubs.acs.org/NanoLett

Nickel–Cobalt Hydroxide Nanosheets Coated on $NiCo_2O_4$ Nanowires Grown on Carbon Fiber Paper for High-Performance Pseudocapacitors

Liang Huang, Dongchang Chen, Yong Ding, Shi Feng, Zhong Lin Wang, and Meilin Liu*

School of Materials Science and Engineering, Georgia Institute of Technology, 771 Ferst Drive, Atlanta, Georgia 30332-0245, United States

Supporting Information

ABSTRACT: A series of flexible nanocomposite electrodes were fabricated by facile electro-deposition of cobalt and nickel double hydroxide (DH) nanosheets on porous $NiCo_2O_4$ nanowires grown radially on carbon fiber paper (CFP) for high capacity, high energy, and power density supercapacitors. Among different stoichiometries of Co_xNi_{1-x}DH nanosheets studied, $Co_{0.67}Ni_{0.33}$ DHs/$NiCo_2O_4$/CFP hybrid nanoarchitecture showed the best cycling stability while maintaining high capacitance of ~1.64 F/cm^2 at 2 mA/cm^2. This hybrid composite electrode also exhibited excellent rate capability; the areal capacitance decreased less than 33% as the current density was increased from 2 to 90 mA/cm^2, offering excellent specific energy density (~33 Wh/kg) and power density (~41.25 kW/kg) at high cycling rates (up to150 mA/cm^2).

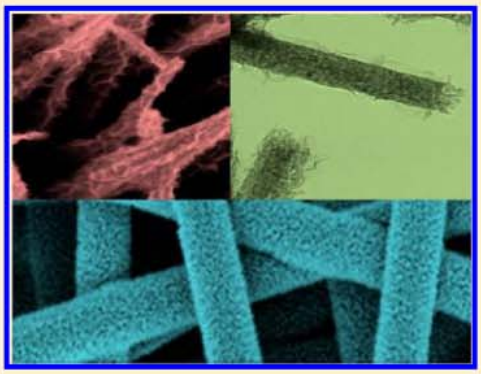

KEYWORDS: *Supercapacitor, $NiCo_2O_4$ nanowire, carbon fiber paper, core/shell, cobalt and nickel hydroxide*

Because of the limited availability of fossil fuel and the increasingly urgent concerns about environmental impact of conventional energy technologies, searching for "green" and renewable energy resources is one of the most pressing challenges facing us today.[1−5,7,8] As one of the most promising type of energy storage device, supercapacitors have attracted more and more attention in recent years. The unique advantages of supercapacitors, also known as electrochemical capacitors, include high-power capability, long cycle lifetime, and fast charge and discharge rates for many applications, from portable electronics to hybrid electric vehicles, and to smart grids .[9,6,10,11] In general, two types of supercapacitors exist based on the underlying energy storage mechanism: electrical double-layer capacitors (EDLCs) and pseudocapacitors. Unlike EDLCs, which store electrical energy by electrostatic accumulation of charges in the electric double-layer near electrode/electrolyte interfaces, pseudocapacitors also make use of reversible Faradaic reactions that occurred at the electrode surface, offering much higher specific capacitance than EDLCs.[12] Transition metal oxides, hydroxides, and their compounds are being widely explored for producing supercapacitors with increased specific capacitance and energy density because of their low cost, low toxicity, and great flexibility in structures and morphology.[13−17] However, their rate capability is usually limited by the inadequate conductivity to support fast electron transport required by high rates. To overcome this problem, most efforts have been focused on using highly conductive carbon materials (such as graphene and carbon nanotubes) as the backbone to support these pseudocapacitive materials,[18−20] significantly enhancing the rate capability of the active materials by shortening the distance of electron transport. However, the tedious fabrication processes and the high cost limit their practical applications.

Three dimensional (3D) hybrid nanostructures with large surface area and short diffusion path for electrons and ions are promising electrode architectures for high-performance supercapacitors. Recently reported hybrid structures such as MnO_2 on Co_3O_4 and $Ni(OH)NO_3$ on CoO supported on a metal substrate showed high specific capacitance and good cycling stability.[21,22] However, the performance of these hybrid materials degraded rapidly as the cycling rate was increased. Since the conductivity of $NiCo_2O_4$ is higher than that of Co_xO_y and NiO, $NiCo_2O_4$ may be used as a backbone to support active electrode materials.[23] Carbon fiber paper (CFP), a network of microsized carbon fibers, has large surface area, high porosity, good electric conductivity, and excellent chemical stability in a wide variety of liquid electrolytes. CFP has been studied extensively as electrode materials or supporting substrate for active materials in fuel cells, batteries, and supercapacitors. Here, we report our findings in design and synthesis of a new 3D hybrid structures of porous cobalt and nickel double hydroxide coatings (Co_xNi_{1-x} DHs) on $NiCo_2O_4$ nanowires directly grown on CFP. This unique nanostructure electrode for pesudocapacitors showed high performance and

Received: March 25, 2013
Revised: May 24, 2013
Published: June 11, 2013

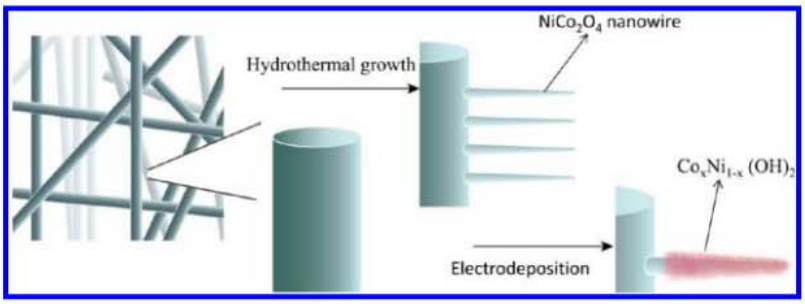

Figure 1. Schematic diagram illustrating the processes for growth $NiCo_2O_4$ nanowires on CFP and subsequent electro-deposition of Co_xNi_{1-x} DHs on the $NiCo_2O_4$ nanowires grown on CFP.

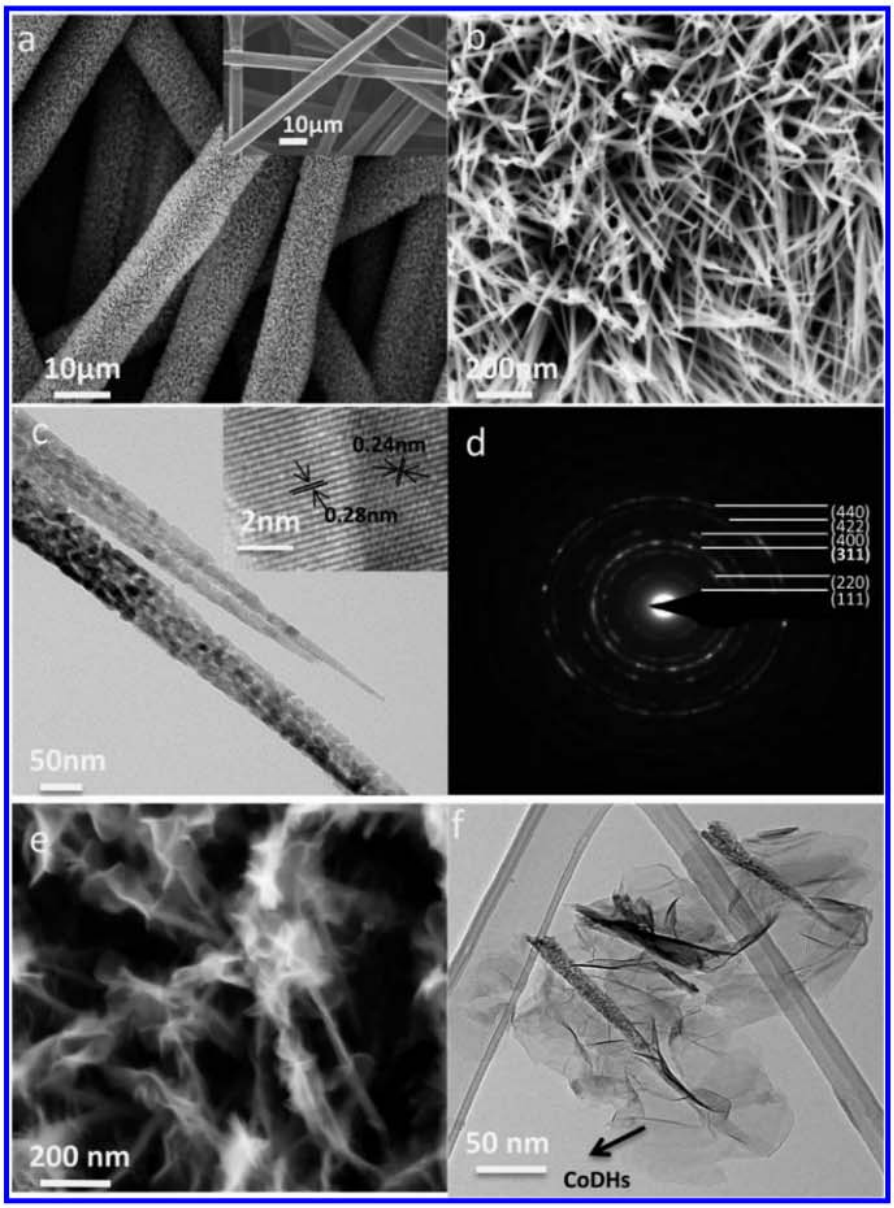

Figure 2. (a) SEM image of CFP before (inset) and after growth of $NiCo_2O_4$ nanowires. (b) High-magnification SEM image of $NiCo_2O_4$ nanowires grown on CFP. (c) TEM image and HRTEM image (inset) of 2 $NiCo_2O_4$ nanowires. (d) Diffraction pattern of a $NiCo_2O_4$ nanowire. (e) SEM image of a CoDHs coating on $NiCo_2O_4$ nanowire grown on CFP. (f) TEM image of CoDHs/$NiCo_2O_4$ nanowires grown on CFP.

excellent rate capability. The crystalline $NiCo_2O_4$ nanowires uniformly grown on CFP were used as the backbone to support and provide reliable electrical connection to the Co_xNi_{1-x} DHs coatings with surface areas accessible to electrolyte, enabling full utilization of the Co_xNi_{1-x} DHs and fast electronic and ionic conduction through the electrode. The $NiCo_2O_4$ may also

dx.doi.org/10.1021/nl401086t | Nano Lett. 2013, 13, 3135−3139

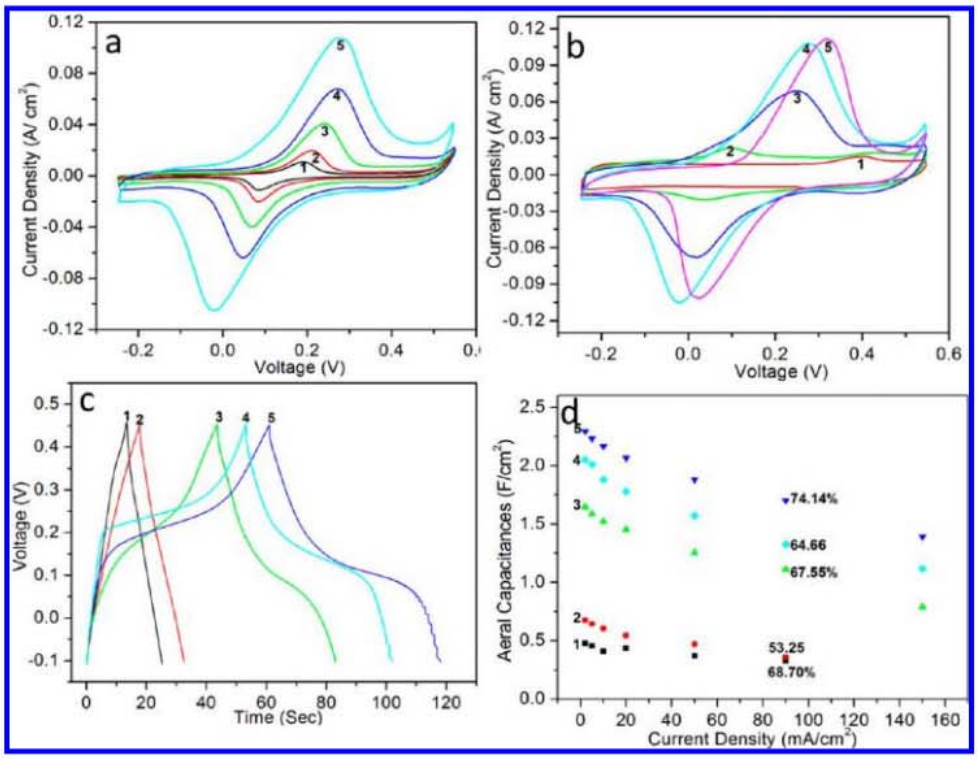

Figure 3. (a) Cyclic voltammograms of a $Co_{0.5}Ni_{0.5}$ DHs/$NiCo_2O_4$/CFP composite electrode in a 3-electrode cell with 1 M KOH aqueous solution at different scan rates: (1) 1 mV/s; (2) 2 mV/s; (3) 5 mV/s; (4) 10 mV/s; (5) 20 mV/s. (b) CVs of $NiCo_2O_4$/CFP and hybrid composite at a scan rate of 20 mV/s: (1) $NiCo_2O_4$/CFP; (2) Co DHs/$NiCo_2O_4$/CFP; (3) $Co_{0.67}Ni_{0.33}$ DHs/$NiCo_2O_4$/CFP; (4) $Co_{0.5}Ni_{0.5}$ DHs/$NiCo_2O_4$/CFP; (5) $Co_{0.33}Ni_{0.67}$ DHs/$NiCo_2O_4$/CFP. (c) Charge and discharge curves of hybrid composite electrodes at a current density of 20 mA/cm^2: (1) $NiCo_2O_4$/CFP; (2) Co DHs/$NiCo_2O_4$/CFP; (3) $Co_{0.67}Ni_{0.33}$ DHs/$NiCo_2O_4$/CFP; (4) $Co_{0.5}Ni_{0.5}$ DHs/$NiCo_2O_4$/CFP; (5) $Co_{0.33}Ni_{0.67}$ DHs/$NiCo_2O_4$/CFP. (d) Areal capacitances of hybrid composite electrodes at different current densities: (1) $NiCo_2O_4$/CFP; (2) Co DHs/$NiCo_2O_4$/CFP; (3) $Co_{0.67}Ni_{0.33}$ DHs/$NiCo_2O_4$/CFP; (4) $Co_{0.5}Ni_{0.5}$ DHs/$NiCo_2O_4$/CFP; (5) $Co_{0.33}Ni_{0.67}$ DHs/$NiCo_2O_4$/CFP.

function as active materials for charge storage and make contribution to the capacitance. The demonstrated areal capacitance (AC) of this hybrid electrode is as high as 2.3 F/cm^2 at a current density of 2 mA/cm^2. It also showed very high rate stability; the areal capacitance decreased less than 40% as the current density was increased from 2 to 150 mA/cm^2. The high capacitance and remarkable rate capability are promising for supercapacitors with both high energy and power densities.

Figure 1 schematically shows the two-step synthesis of the hybrid structure: (1) hydrothermal growth of $NiCo_2O_4$ nanowires on CFP and (2) electro-deposition of a thin Co_xNi_{1-x} DHs coating on the $NiCo_2O_4$ nanowire arrays. The hydrothermally synthesized $NiCo_2O_4$ nanowire arrays serve as the backbone for the subsequent deposition of Co_xNi_{1-x} DH nanosheets.

$NiCo_2O_4$ nanowire arrays aligned on the carbon fiber were fabricated by a facile modified hydrothermal process.[24] Figure 2a,b shows the morphology and microstructure of the $NiCo_2O_4$ nanowires on CFP. It is revealed that high-density $NiCo_2O_4$ nanowires were radially grown on the CFP with the length of ~3 μm and diameter of 30−80 nm. After electro-deposition, the $NiCo_2O_4$ nanowires are decorated with Co_xNi_{1-x} DHs coatings (Figure 2e and Supporting Information Figure SI1a,b). The $NiCo_2O_4$ wire can be distinguished from the Co_xNi_{1-x} DHs coating under a TEM. (Figure 2f and Supporting Information Figure SI1c−e) The $NiCo_2O_4$ nanowires are highly porous and composed of 10−20 nm nanocrystallites with pores of 2−4 nm in diameter (Figure 2c). The selected-area electron diffraction (SAED) pattern and HRTEM image show that the mesoporous $NiCo_2O_4$ nanowires are polycrystalline (Figure 2d). The Co_xNi_{1-x} DH thin film coatings on the surface of $NiCo_2O_4$ nanowires have a thickness of several nanometers. The spatial distributions of the elements in the shell structures were characterized using energy-dispersive spectroscopy (EDS) in the form of line scan profiles of individual elements (Co, Ni, and O), as shown in Supporting Information Figure SI1d−f. The X-ray diffraction pattern shows that the hybrid structure contains cubic $NiCo_2O_4$ with a space group of *Fd*3*m* (JCPDS Card No.73-1702), □-$Co(OH)_2$ and □-$Ni(OH)_2$ phase (JCPDS 74-1057 and 38-0715) (Figure SI2 Supporting Information). Because of the unique microstructure with huge specific area, the 3D $NiCo_2O_4/Co_xNi_{1-x}$ DHs architecture has a potential to significantly enhance the electrochemical performance of the $NiCo_2O_4/Co_xNi_{1-x}$DHs/CFP hybrid composite electrode.

Further, Raman spectroscopy was also used to characterize the phase composition of the $NiCo_2O_4/Co_xNi_{1-x}$ DHs core/shell structure. As seen in Supporting Information Figure SI3, the peaks at 186, 456, 504, and 648 cm^{-1} correspond to F_{2g}, E_g F_{2g}, and A_{1g} modes of the $NiCo_2O_4$ nanowires, respectively.[25] After electro-deposition of a $Co_{0.5}Ni_{0.5}$DHs coating, a new peak at 458 cm^{-1} was observed, corresponding to the stretching Ni−O (H) bond, and another one at 525 cm^{-1}, attributed to the Co−O (A_g) symmetric stretching mode.[26,27]

We then investigate the electrochemical properties of the Co_xNi_{1-x}DHs/$NiCo_2O_4$/CFP electrodes in a three-electrode cell with 1 M KOH electrolyte using cyclic voltammetry (CV) and charge−discharge cycling (Figure 3a and Supporting

dx.doi.org/10.1021/nl401086t | Nano Lett. 2013, 13, 3135 3139

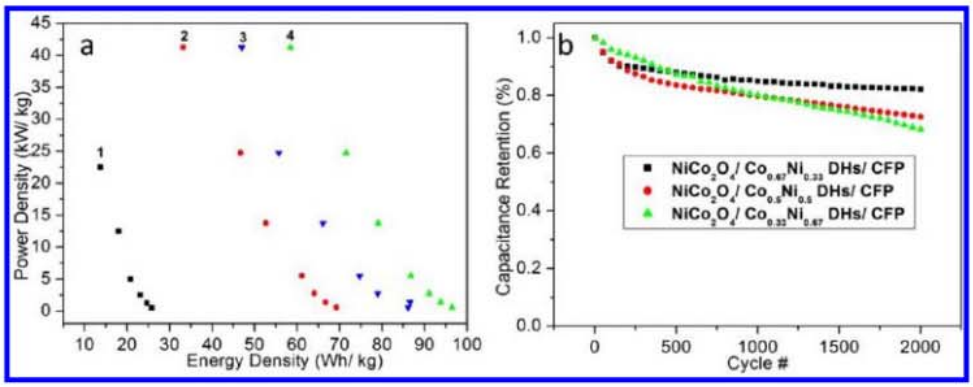

Figure 4. (a) Specific energy and power density of Co_xNi_{1-x} DHn/$NiCo_2O_4$/CFP electrodes evaluated at different charge/discharge rates (current densities); (1) Co DHs/$NiCo_2O_4$/CFP; (2) $Co_{0.67}Ni_{0.33}$ DHs/$NiCo_2O_4$/CFP; (3) $Co_{0.5}Ni_{0.5}$ DHs/$NiCo_2O_4$/CFP; (4) $Co_{0.33}Ni_{0.67}$ DHs/$NiCo_2O_4$/CFP. (b) Capacity retention of the hybrid composite electrodes evaluated at a constant charge/discharge cycling rate of 2 mA/cm^2.

Information Figure SI4). Figure 3b shows some typical CV curves at scan rate of 20 mV/s in a potential window of −0.25 to 0.55 V for a hybrid electrode with Co_xNi_{1-x} DHs by electrodeposition for 7 min. The $NiCo_2O_4$ nanowires on CFP ($NiCo_2O_4$/CFP) showed a weak redox peak at 0.3−0.4 V, suggesting poor electrochemical performance of $NiCo_2O_4$ nanowires. In contrast, the $NiCo_2O_4$ nanowires coated with a $Co(OH)_2$ coating showed a redox peak at 0.1 V, corresponding to the redox reaction described by eq 1. After doping Ni into the $Co(OH)_2$ coating, the redox peak was significantly enhanced. Further, the anodic peaks in the CV curves shifted to a more positive potential with the increasing Ni content in the Co_xNi_{1-x} DHs coating, consistent with a previous report.[25] The redox peaks of the Co_xNi_{1-x} DHs originated mainly from the Faradaic reactions of the surface oxycation species. In the alkaline electrolyte, these reactions involve the redox transitions of hydrous nickel and cobalt oxide based on the equations[16,28]

$$Co(OH)_2 + OH^- \rightleftharpoons CoOOH + H_2O + e^- \quad (1)$$

$$CoOOH + OH^- \rightleftharpoons CoO_2 + H_2O + e^- \quad (2)$$

$$Ni(OH)_2 + OH^- \rightleftharpoons NiOOH + H_2O + e^- \quad (3)$$

Rate capability is a critical parameter for supercapacitors that may limit the applicability to many applications. Shown in Supporting Information Figure SI5 is some typical galvanostatic charge/discharge cycling curves of the as-prepared, 3D Co_xNi_{1-x}DHs/$NiCo_2O_4$/CFP hybrid electrodes at different current densities. These curves are symmetric, indicating that the hybrid composite has a good electrochemical capacitive characteristic and superior reversible redox reaction. The cycling curves are still symmetrical even at a current density as high as 150 mA/cm^2, an indication of very high rate stability. The areal capacitance (F/cm^2) is calculated from the following equation

$$C = \frac{Jt}{\Delta V}$$

where J is the current density (A/cm^2), t is the discharge time (s), and ΔV is the voltage window (V) for the cycling test. The discharge areal capacitance of the 3D Co_xNi_{1-x}DHs/$NiCo_2O_4$/CFP hybrid composite electrodes at 10 mA/cm^2 is 0.61, 1.52, 2.17, and 1.88 F/cm^2 for x = 1, 0.67, 0.5, and 0.33, respectively. These capacity values are about 1.5, 3.7, 5.3, and 4.6 times the capacitance of electrode based on pristine $NiCo_2O_4$ nanowire arrays grown on CFP. These results suggest that ordered hybrid architecture of the pseudocapacitive materials many enhance capacitance. The areal capacitances at different current densities are shown in Figure 3d. Among the different ratios of Co to Ni in the Co_xNi_{1-x} DHs materials, the hybrid composite with a $Co_{0.5}Ni_{0.5}$ DHs coating has the highest areal capacitance (~2.3 F/cm^2) at a current density 2 mA/cm^2. The hybrid arrays still have an areal capacitance of ~1.4 F/cm^2 when the current density was increased to 150 mA/cm^2, implying that it can retain ~60.8% of its initial value when the current density was increased by 75 times. For the hybrid composite with a $Co_{0.33}Ni_{0.67}$ DHs coating, the capacity retention is ~67.5% when the current density was increased from 2 to 90 mA/cm^2. From an even higher current density of 10 to 150 mA/cm^2, it still retained ~51.9% of the initial capacity, which is superior to that of previous report about the nickel hydroxidenitrate-ZnO nanowire heterostructure that showed a capacitance retention of 42% when the current density increase from 15.7 to 157.2 A/g.[29] The capacity retention of hybrid composite with $Co_{0.67}Ni_{0.33}$ DHs is ~53% at a current density as high as 150 mA/cm^2. In addition, the specific capacitances of these three hybrid electrodes are all over 1500 F/g at current density of 2 mA/cm^2 (Supporting Information Figure SI6).

Since it is vital to retain high specific capacitances (or energy density) at high current density for many applications, we estimated the energy and power density of our Co_xNi_{1-x}DHs/$NiCo_2O_4$/CFP based supercapacitors under different operating conditions. As shown in the Ragone plot (Figure 4a), the hybrid composite with $Co_{0.5}Ni_{0.5}$DHs delivered an energy density of ~58.4 Wh/kg at a power density of ~41.3 kW/kg. For the hybrid composite with $Co_{0.67}Ni_{0.33}$ DHs and $Co_{0.33}Ni_{0.67}$ DHs, the highest specific power density was ~41.3 kW/kg with an energy density of ~33.2 Wh/kg and ~47 Wh/kg, respectively. These results are superior to those reported for the single crystalline $Ni(OH)_2$ grown on graphene sheets.[19] In addition, the specific power density 41.3 kW/kg may meet the power demand of the PNGV (Partnership for a New Generation of Vehicles)[30] for hybrid vehicle systems.

The cycling life of the 3D Co_xNi_{1-x}DHs/$NiCo_2O_4$/CFP hybrid composite electrodes was evaluated at a current density of 2 mA/cm^2 in the potential range of −0.1 to 0.45 V for more than 2000 cycles, as shown in Figure 4b. Hybrid electrode with the $Co_{0.66}Ni_{0.33}$ DHs coating has better cycling stability than the one with a $Co_{0.5}Ni_{0.5}$ DHs or $Co_{0.33}Ni_{0.66}$ DHs coating. For the hybrid electrode with a $Co_{0.66}Ni_{0.33}$ DHs coating, the capacitance decreased gradually ~10% at the 200th cycle, and

dx.doi.org/10.1021/nl401086t | Nano Lett. 2013, 13, 3135−3139

then declined another ~8.7% after additional 1800 cycles. The total capacitance loss after 2000 cycles is ~18.7%, which is lower than that reported for a single phase $Co(OH)_2$ and $Ni(OH)_2$ grown on nickel foam tested under similar conditions.[31,32] For the hybrid electrode with a $Co_{0.5}Ni_{0.5}$ DHs and $Co_{0.33}Ni_{0.66}$ DHs coating, the total capacitance loss after 2000 cycles is ~28 and ~32%, much worse than that for the one with a $Co_{0.66}Ni_{0.33}$ DHs coating.

Clearly, the 3D $Co_{0.66}Ni_{0.33}$ DHs/$NiCo_2O_4$/CFP hybrid composite seems to be the most promising one among the compositions studied. While it does not show the highest electrochemical performance, its high rate capability and excellent cycling stability make it more suitable for practical applications. The high performance of the hybrid composite electrodes is attributed to the following unique features of the electrode. First, the high conductivity of CFP with appropriate pore channels allows efficient current collection and rapid access to the surfaces of the electrochemically active materials. Second, the porous $NiCo_2O_4$ nanowire and the ultrathin coating of Co_xNi_{1-x} DHs offer large surface area with short electrons and ions diffusion path, thus leading to faster kinetics and higher utilization of active material.

In conclusion, we have designed and prepared 3D Co_xNi_{1-x}DHs/$NiCo_2O_4$/CFP hybrid composite electrodes using a facile hydrothermal synthesis and an electrodeposition process. These hybrid composite electrodes exhibit high performance in a three-electrode cell. Among the different ratios of cobalt to nickel in the coating materials, $Co_{0.66}Ni_{0.33}$ DHs offers high energy and power density as well as better cycling life. Furthermore, the unique nanoarchitecture of this hybrid electrode may be applicable to other chemical and energy transformation processes such as lithium ion batteries, water splitting, photodetector, and nonenzymatic biosensors.

ASSOCIATED CONTENT

Supporting Information

Additional information and figures. This material is available free of charge via the Internet at http://pubs.acs.org.

AUTHOR INFORMATION

Notes

The authors declare no competing financial interest.

ACKNOWLEDGMENTS

This material is based upon work supported as part of the Heterogeneous Functional Materials (HetroFoaM) Center, an Energy Frontier Research Center funded by the U.S. Department of Energy, Office of Science, Office of Basic Energy Sciences under Award Number DE-SC0001061. L.H. thanks for a fellowship from the China Scholarship Council.

REFERENCES

(1) Tian, B.; Zheng, X.; Kempa, T. J.; Fang, Y.; Yu, N.; Yu, G.; Huang, J.; Lieber, C. M. *Nature* **2007**, *449*, 885.
(2) Wang, X. D.; Song, J. H.; Liu, J.; Wang, Z. L. *Science* **2007**, *316*, 102.
(3) Chan, C.; Peng, H.; Liu, G.; Mcilwrath, K.; Zhang, X.; Huggins, R.; Cui, Y. *Nat. Nanotechnol.* **2008**, *3*, 31.
(4) Wang, Z. L.; Song, J. H. *Science* **2006**, *312*, 242.
(5) Xia, C.; Liu, M. L. *Adv. Mater.* **2002**, *4*, 521.
(6) Dresselhaus, M. S.; Thomas, I. L. *Nature* **2001**, *414*, 332.
(7) Bae, J.; Song, M. K.; Park, Y. J.; Kim, J. M.; Liu, M. L.; Wang, Z. L. *Angew. Chem., Int. Ed.* **2011**, *50*, 1683.
(8) Gur, I.; Fromer, N. A.; Geier, M. L.; Alivisatos, A. P. *Science* **2005**, *310*, 462.
(9) Simon, P.; Gogotsi, Y. *Nat. Mater.* **2008**, *7*, 845.
(10) Miller, J. R.; Simon, P. *Science* **2008**, *321*, 651.
(11) Hall, P. J.; Mirzaeian, M.; Fletcher, S. I.; Sillars, F. B.; Rennie, A. J. R.; Shitta-Bey, G. O.; Wilson, G.; Cruden, A.; Carter, R. *Energy. Environ. Sci.* **2010**, *3*, 1238.
(12) Sarangapani, S.; Tilak, B. V.; Chen, C.-P. *J. Electrochem. Soc.* **1996**, *143*, 3761.
(13) Yang, L.; Cheng, S.; Ding, Y.; Zhu, X.; Wang, Z. L.; Liu, M. L. *Nano Lett.* **2012**, *12*, 321.
(14) Song, M. K.; Cheng, S.; Chen, H.; Qin, W. T.; Nam, K. W.; Xu, S.; Yang, X. Q.; Bongiorno, A.; Lee, J.; Bai, J.; Tyson, T. A.; Cho, J.; Liu, M. L. *Nano Lett.* **2012**, *12*, 3483.
(15) Meng, C. Z.; Liu, C. H.; Fan, S. S. *Electrochem. Commun.* **2009**, *11*, 186.
(16) Wang, X.; Sumboja, A.; Lin, M.; Yan, J.; Lee, P. S. *Nanoscale.* **2012**, *4*, 7266.
(17) Yuan, C. Z.; Yang, L.; Hou, L.; Shen, L. F.; Zhang, X. G.; Lou, X. W. *Energy. Environ. Sci.* **2012**, *5*, 883.
(18) Yan, J.; Fan, Z.; Wei, T.; Qian, W.; Zhang, M. L.; Wei, F. *Carbon* **2010**, *48*, 3825.
(19) Wang, H. L.; Casalongue, H. S.; Liang, Y.; Dai, H. J. *J. Am. Chem. Soc.* **2010**, *132*, 7472.
(20) Hou, Y.; Cheng, Y. W.; Hobson, T.; Liu, J. *Nano Lett.* **2010**, *10*, 2727.
(21) Guan, C.; Liu, J. P.; Cheng, C. W.; Li, H. X.; Li, X. L.; Zhou, W.; Zhang, H.; Fan, H. J. *Energy. Environ. Sci.* **2011**, *4*, 4496.
(22) Liu, J. P.; Jiang, J.; Cheng, C.; Li, H. X.; Zhang, J.; Gong, H.; Fan, H. J. *Adv. Mater.* **2011**, *23*, 2076.
(23) Wei, T. Y.; Chen, C. H.; Chien, H. C.; Lu, S. Y.; Hu, C. C *Adv. Mater.* **2010**, *22*, 347.
(24) Wang, Q. F.; Liu, B.; Wang, X. F.; Ran, S.; Wang, L.; Chen, D.; Shen, G. Z. *J. Mater. Chem.* **2012**, *22*, 21647.
(25) Liu, Z. Q.; Xiao, K.; Xu, Q. Z.; Li, N.; Su, Y. Z.; Wang, H. J.; Chen, S. *R. Soc. Chem. Adv.* **2013**, *3*, 4372.
(26) Vidotti, M.; Salvador, R. P.; Torresi, S. I. C *Ultrasonics Sonochem.* **2009**, *16*, 35.
(27) Yang, J.; Liu, H. W.; Martens, W. N.; Frost, R. L. *J. Phys. Chem. C.* **2010**, *114*, 111.
(28) Gupta, V.; Gupta, S.; Miura, N. *J. Power. Sources.* **2008**, *175*, 680.
(29) Liu, J. P.; Cheng, C. W.; Zhou, W.; Lia, H. X.; Fan, H. J. *Chem. Commun.* **2011**, *47*, 3436.
(30) Scrosati, B. *Nature* **1995**, *373*, 557.
(31) Xia, X. H.; Tu, J. P.; Zhang, Y. Q.; Mai, Y. J.; Wang, X. L.; Gu, C. D.; Zhao, X. B. *J. Phys. Chem. C.* **2011**, *115*, 22662.
(32) Yang, G. W.; Xu, C. L.; Li, H. L. *Chem. Commun.* **2008**, 6537.